

Article

# Dynamic Mechanical Relaxation in LaCe-Based Metallic Glasses: Influence of the Chemical Composition

Minna Liu <sup>1</sup>, Jichao Qiao <sup>1,\*</sup>, Qi Hao <sup>1</sup>, Yinghong Chen <sup>1</sup>, Yao Yao <sup>1</sup>, Daniel Crespo <sup>2</sup>  and Jean-Marc Pelletier <sup>3</sup>

<sup>1</sup> School of Mechanics, Civil Engineering Architecture, Northwestern Polytechnical University, Xi'an 710072, China; liuminna@mail.nwpu.edu.cn (M.L.); haoq@mail.nwpu.edu.cn (Q.H.); cyhongc@mail.nwpu.edu.cn (Y.C.); yaoy@nwpu.edu.cn (Y.Y.)

<sup>2</sup> Departament de Física, Barcelona Research Center in Multiscale Science and Technology & Institut de Tècniques Energètiques, Universitat Politècnica de Catalunya, 08930 Barcelona, Spain; Daniel.Crespo@upc.edu

<sup>3</sup> MATEIS, UMR CNRS5510, Bat. B. Pascal, INSA-Lyon, F-69621 Villeurbanne CEDEX, France; jean-marc.pelletier@insa-lyon.fr

\* Correspondence: qjczy@nwpu.edu.cn

Received: 13 August 2019; Accepted: 14 September 2019; Published: 17 September 2019



**Abstract:** The mechanical relaxation behavior of the  $(La_{0.5}Ce_{0.5})_{65}Al_{10}(Co_xCu_{1-x})_{25}$  at% ( $x = 0, 0.2, 0.4, 0.6,$  and  $0.8$ ) metallic glasses was probed by dynamic mechanical analysis. The intensity of the secondary  $\beta$  relaxation increases along with the Co/Cu ratio, as has been reported in metallic glasses where the enthalpy of mixing for all pairs of atoms is negative. Furthermore, the intensity of the secondary  $\beta$  relaxation decreases after physical aging below the glass transition temperature, which is probably due to the reduction of the atomic mobility induced by physical aging.

**Keywords:** metallic glasses; mechanical spectroscopy; mixing enthalpy; Kohlrausch–Williams–Watts equation; structural heterogeneity

## 1. Introduction

Metallic glasses (MGs) have been extensively studied for several decades because they exhibit unique physical, chemical and mechanical properties and have no crystal defects (i.e., dislocations, grain boundaries, and vacancies) [1–3]. Compared to other glassy materials (i.e., amorphous polymers, oxide glasses, and other non-crystalline solids), metallic glasses show high yield strength and resilience, large fracture toughness, and attractive corrosion resistance [4–8]. It is well known that the mechanical and physical properties of metallic glasses, i.e., plasticity, glass transition behavior, and diffusion phenomena, are bound up with their mechanical relaxation modes [1,6,9–11]. Nevertheless, below the glass transition temperature, metallic glasses have insufficient ductility due to shear band instability during plastic deformation, which dramatically reduces the use in structural applications [12]. Compared to crystalline metals, metallic glasses are basically characterized by brittleness at room temperature. One way to overcome the macroscopic brittle behavior of metallic glass is to reduce the size. Previous studies have shown that brittle behavior can be mitigated when the sample size is reduced to sub-micron levels, thereby reducing the effects of instability on material behavior [13,14]. Below the glass transition, metallic glasses are thermodynamically in a non-equilibrium state, as there is a large enthalpy difference from the crystallized state [15]. However, the topological structure as well as the physical mechanism of relaxation in glassy materials remain unresolved issues [16–18].

In the supercooled liquid phase region of metallic glasses, relaxation processes drive the glass towards more stable states. The primary  $\alpha$  relaxation and secondary  $\beta$  relaxation are considered the elementary relaxation processes [19–21]. Johari et al. [22] proposed that glasses and glass-forming liquids have two relaxation modes: (i) The primary ( $\alpha$ ) relaxation, which is a global, structural atomic or molecular rearrangement observed at relatively high temperatures and closely related to the glass transition phenomenon; (ii) The secondary ( $\beta$ ) relaxation, a low energy process which is observed under the glass transition temperature  $T_g$ . While the  $\alpha$  relaxation process shows a complex dependence on temperature, the secondary  $\beta$  relaxation generally submits to an Arrhenius temperature dependence rule. The  $\beta$  relaxation shows up as an over wing in the high-frequency tail or a side shoulder at low temperature of  $\alpha$  relaxation [23,24]. Contrary to the main relaxation,  $\beta$  relaxation is associated with the motion of atoms or molecules inside a glass material without topological rearrangement. The study on the connection between the diffusion behavior of the amorphous alloy, plastic deformation, and glass transition on the relaxation process of amorphous alloy is of great significance for the assessment of the potential applications of metallic glasses.

Literature results show that La-based metallic glasses display a conspicuous secondary relaxation [25]. Therefore, La-based metallic glasses are an ideal model system to investigate the relaxation process. In the present study, the dynamic mechanical properties of emblematic LaCe-based metallic glasses were investigated by mechanical spectroscopy. The physical mechanism of mechanical relaxation process was analyzed relied on the Kohlrausch–Williams–Watts (KWW) equation.

## 2. Experimental Procedure

The  $(\text{La}_{0.5}\text{Ce}_{0.5})_{65}\text{Al}_{10}(\text{Co}_x\text{Cu}_{1-x})_{25}$  at% ( $x = 0, 0.2, 0.4, 0.6$  and  $0.8$ ) precursor alloy was produced by arc melting in high-purity argon atmosphere, after titanium melting for the removal of residual oxygen. The alloy was re-melted at least four times to ensure chemical homogeneity. Suction casting copper method was eventually used to produce plates of 2 mm thickness.

The structural properties of the samples were checked by X-ray diffraction (XRD, Philips PW 3830, Amsterdam, Netherlands) using monochromatic Cu-K $\alpha$  radiation. The glass transition  $T_g$  and crystallization onset  $T_x$  temperatures were determined by differential scanning calorimeter (DSC, NEZTCH 404 C, Bavaria, Germany) at a heating rate of 10 K/min. Dynamical mechanical analysis (DMA, TA Q800, USA) was used to monitor the mechanical relaxation behavior. Samples of 30 mm (length)  $\times$  2 mm (width)  $\times$  1 mm (thickness) for DMA analysis were produced on a precise water-cooled low-speed cutting machine. DMA measurements were performed on single cantilever, at a 3 K/min heating rate; the complex elastic modulus is denoted as  $E$  (storage modulus  $E'$  and the loss modulus  $E''$ ).

## 3. Experimental Results and Discussions

### 3.1. Structural and Thermal Properties

The amorphous nature of  $(\text{La}_{0.5}\text{Ce}_{0.5})_{65}\text{Al}_{10}(\text{Co}_x\text{Cu}_{1-x})_{25}$  at% ( $x = 0, 0.2, 0.4, 0.6$  and  $0.8$ ) was confirmed by XRD. XRD patterns of  $(\text{La}_{0.5}\text{Ce}_{0.5})_{65}\text{Al}_{10}(\text{Co}_x\text{Cu}_{1-x})_{25}$  at% ( $x = 0, 0.2, 0.4, 0.6$ , and  $0.8$ ) bulk metallic glasses, as presented in Figure 1a, exhibit broad diffraction peaks, and no traces of crystalline phases are detected. Therefore, the glassy nature of the  $(\text{La}_{0.5}\text{Ce}_{0.5})_{65}\text{Al}_{10}(\text{Co}_x\text{Cu}_{1-x})_{25}$  at% ( $x = 0, 0.2, 0.4, 0.6$ , and  $0.8$ ) bulk metallic glasses (BMG) was verified.

DSC curves of the  $(\text{La}_{0.5}\text{Ce}_{0.5})_{65}\text{Al}_{10}(\text{Co}_x\text{Cu}_{1-x})_{25}$  at% ( $x = 0, 0.2, 0.4, 0.6$  and  $0.8$ ) bulk metallic glasses are presented in Figure 1b. The main thermal events are the glass transition and subsequent crystallization. The glass transition temperatures  $T_g$ , indicated by arrows in the figure, increase almost linearly with the substitution of Copper by Cobalt. While the Co-free  $(\text{La}_{0.5}\text{Ce}_{0.5})_{65}\text{Al}_{10}\text{Cu}_{25}$  alloy has a glass transition temperature of 372 K, the  $T_g$  of  $(\text{La}_{0.5}\text{Ce}_{0.5})_{65}\text{Al}_{10}(\text{Co}_{0.8}\text{Cu}_{0.2})_{25}$  alloy increases up to 404 K. Crystallization temperatures  $T_x$  show a less predictable behavior. Given that the difference between the crystallization and glass transition temperatures is a parameter largely related to the

glass stability, it is observed that  $(\text{La}_{0.5}\text{Ce}_{0.5})_{65}\text{Al}_{10}(\text{Co}_{0.2}\text{Cu}_{0.8})_{25}$  metallic glass is the most stable glass. The XRD patterns and DSC curves corroborate the amorphous properties of the studied alloys.

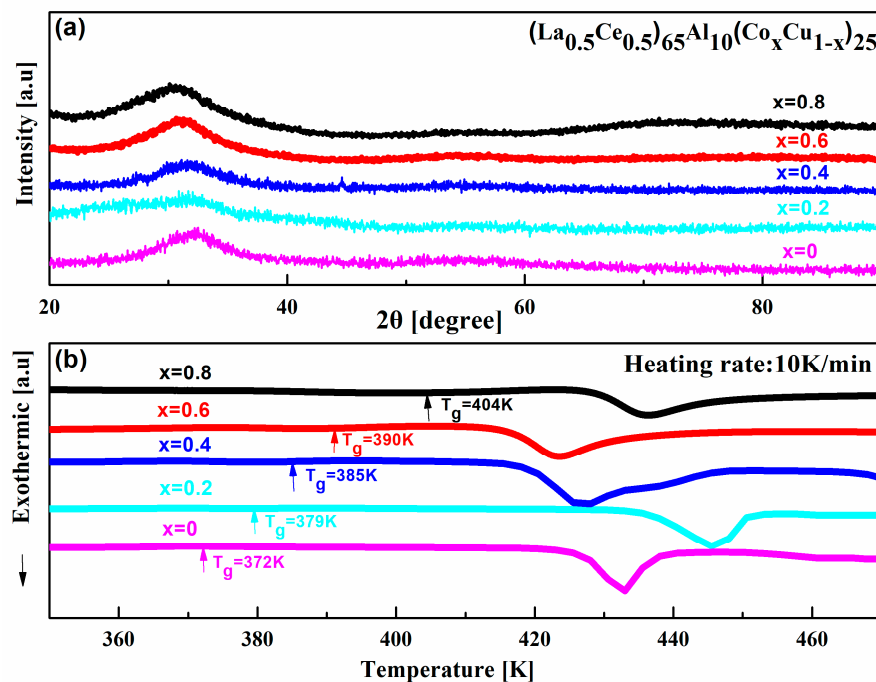


**Figure 1.** (a) XRD patterns of the  $(\text{La}_{0.5}\text{Ce}_{0.5})_{65}\text{Al}_{10}(\text{Co}_x\text{Cu}_{1-x})_{25}$  at% ( $x = 0, 0.2, 0.4, 0.6,$  and  $0.8$ ), as-cast state. (b) Differential scanning calorimeter (DSC) curves of the  $(\text{La}_{0.5}\text{Ce}_{0.5})_{65}\text{Al}_{10}(\text{Co}_x\text{Cu}_{1-x})_{25}$  at% ( $x = 0, 0.2, 0.4, 0.6,$  and  $0.8$ ) at a heating rate of 10 K/min. The glass transition temperature  $T_g$  of the different metallic glasses is pointed out in the figure.

### 3.2. Dynamic Mechanical Analysis

#### 3.2.1. Constant Frequency Measurements

Dynamic mechanical analysis is very sensitive to the atomic and molecular mobility of amorphous materials. The  $(\text{La}_{0.5}\text{Ce}_{0.5})_{65}\text{Al}_{10}(\text{Co}_{0.4}\text{Cu}_{0.6})_{25}$  metallic glass dynamic mechanical response was measured from room temperature to 550 K with a heating rate of 3 K/min and a driving frequency of 1 Hz. Figure 2 exhibits the normalized storage modulus  $E'$  and loss modulus  $E''$  as a function of temperature, where  $E_u$  represents the unrelaxed modulus at room temperature. The temperature dependence of  $E'$  and  $E''$  is very similar to most other BMGs [9,26,27]. It is worth noticing that when the temperature is below the  $T_g$ , loss modulus curve showed no apparent  $\beta$  relaxation [9,28,29]. The storage modulus and loss modulus of the LaCe-based metallic glass vary with temperature, and the process can be segmented into three different regions:

Region (I): In the low temperature region, i.e., beneath 350 K, the normalized storage modulus is large and close to unity. Contrarily, the loss modulus  $E''$  is negligible. Therefore, the glassy material mainly exhibits elastic deformation in this temperature range, and the viscoelastic component can be neglected.

Region (II): The medium temperature region comprises the temperature range of 390 K to 460 K. A large increase of the loss modulus  $E''$  is observed reaching a peak at the temperature  $T_\alpha$ , denoting the  $\alpha$  relaxation characteristic of amorphous materials. This process is the dynamic glass transition. The storage modulus  $E'$  starts to diminish while the loss modulus  $E''$  boosts. This temperature range falls within the super-cooled liquid region of metallic glasses.

Region (III): The high temperature region starts at 460 K. The storage modulus  $E'$  increases again reaching a value similar to that at room temperature, due to crystallization. The loss modulus  $E''$  falls to a relatively low value.

As shown in Figure 2, the  $\beta$  relaxation is not observed below  $T_g$  [22,23].  $\beta$  relaxation in this glass should be found in the temperature range from 300 to 400 K.

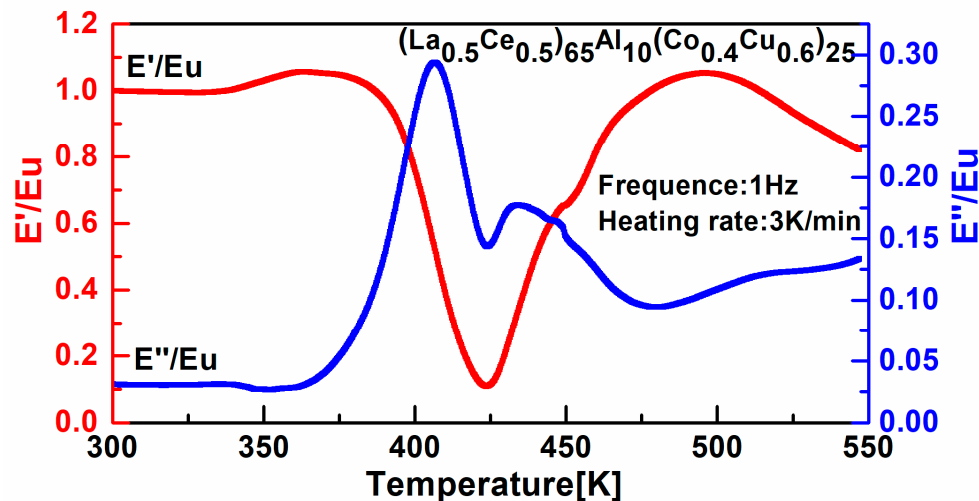


**Figure 2.** Thermal dependence of the normalized storage  $E'/E_u$  and loss modulus  $E''/E_u$  of  $(\text{La}_{0.5}\text{Ce}_{0.5})_{65}\text{Al}_{10}(\text{Co}_{0.4}\text{Cu}_{0.6})_{25}$  metallic glass. Measurement was carried out at a fixed frequency of 1 Hz and a heating rate of 3 K/min.  $E_u$  is the unrelaxed modulus, which equals the value of  $E'$  at room temperature.

Figure 3 exhibits the normalized dynamic loss modulus  $E''$  as a function of temperature at a constant frequency (1 Hz) in  $(\text{La}_{0.5}\text{Ce}_{0.5})_{65}\text{Al}_{10}(\text{Co}_x\text{Cu}_{1-x})_{25}$  at% ( $x = 0, 0.2, 0.4, 0.6,$  and  $0.8$ ) glass alloys. The data are normalized to the values of temperature and loss modulus at the peak of the  $\alpha$  relaxation, namely  $T_\alpha$  and  $E''_{max}$ . Interestingly, the secondary relaxation process depends significantly on the chemical composition of the glass. The intensity of  $\beta$  relaxation of  $(\text{La}_{0.5}\text{Ce}_{0.5})_{65}\text{Al}_{10}(\text{Co}_x\text{Cu}_{1-x})_{25}$  at% ( $x = 0, 0.2, 0.4, 0.6,$  and  $0.8$ ) decreases with the increase of the Cu content. The behavior of the loss module reveals a noticeable change in the features of the  $\beta$  relaxation around  $0.8 T_g$  for the different compositions. For  $(\text{La}_{0.5}\text{Ce}_{0.5})_{65}\text{Al}_{10}\text{Cu}_{25}$  metallic glass, the  $\beta$  relaxation merely declares as a weak shoulder. It is significant that in several metallic glasses that exhibit an evident  $\beta$  relaxation, this has been correlated to plasticity [30]. It has also been proven that the mechanical relaxation process, especially the  $\beta$  relaxation, is sensitive to the micro-alloying in metallic glasses.

Previous works indicate that the  $\beta$  relaxation reflects the inherent structural heterogeneities in metallic glasses, described for instance as soft domains, liquid-like regions, local topological structure of loose packing regions, and flow units [1]. In the current study, minor addition of Cobalt in the  $(\text{La}_{0.5}\text{Ce}_{0.5})_{65}\text{Al}_{10}(\text{Co}_x\text{Cu}_{1-x})_{25}$  at% ( $x = 0, 0.2, 0.4, 0.6,$  and  $0.8$ ) bulk metallic glasses is very important and reshapes the relaxation mode (i.e.,  $\beta$  relaxation).

In order to associate the different behavior of  $\beta$  relaxation and the deformability of metallic glass with its structure, transmission electron microscopy (TEM) was carried out to reveal the microstructural characteristics of metallic glass [31]. The most notable structural feature is that the metallic glass is composed of two types of regions: Light regions with typical sizes ranging from 50 to 200 nm are enveloped by dark boundary regions, which are about 5–20 nm in width. It was further confirmed that both of the two regions are of a glassy nature. It is proposed that the local atomic motions of soft regions are responsible for  $\beta$  relaxations, and the heterogeneous structure improves the plasticity of metallic glasses though the formation of multiple shear bands [32].

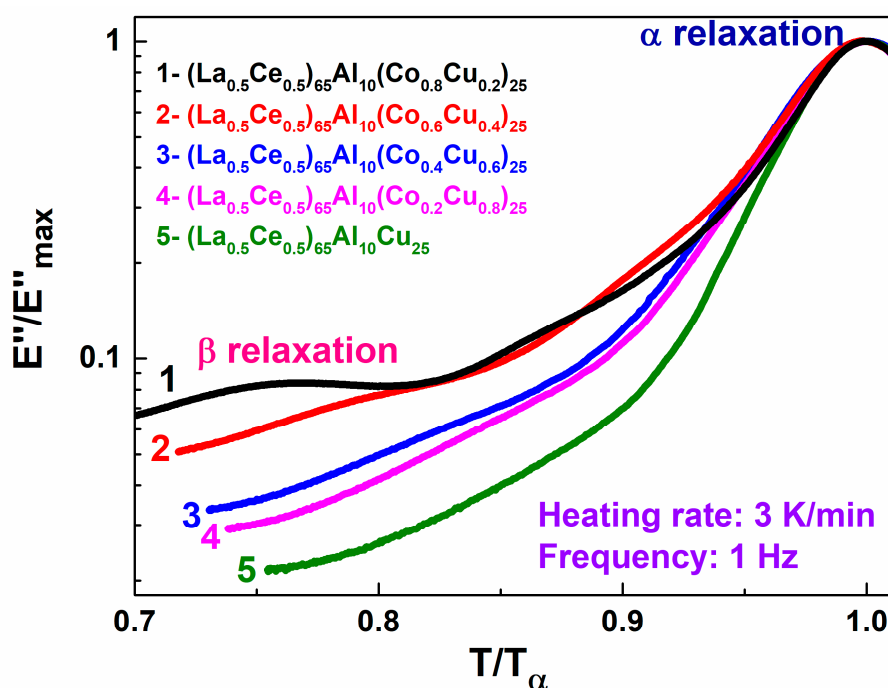


**Figure 3.** Temperature dependence of the loss modulus  $E''/E''_{max}$  in the  $(La_{0.5}Ce_{0.5})_{65}Al_{10}(Co_xCu_{1-x})_{25}$  at% ( $x = 0, 0.2, 0.4, 0.6, 0.8$ ) metallic glass (Heating rate: 3 K/min; frequency: 1 Hz).

The relationship between enthalpy of mixing and  $\beta$  relaxation can be used to qualitatively anticipate the intensity  $\beta$  relaxation of some metallic glasses [33]. An empirical rule on  $\beta$  relaxation has been established [34]: Pronounced  $\beta$  relaxation is associated with alloys where all the atomic pairs have larger and similar negative values of the mixing enthalpy. On the other hand, positive or large fluctuations in the values of mixing enthalpy reduce and even suppress  $\beta$  relaxation [33].

Regarding the  $\beta$  relaxation in  $(La_{0.5}Ce_{0.5})_{65}Al_{10}(Co_xCu_{1-x})_{25}$  at% metallic glasses, the features of the mixing enthalpy between the constituent atoms correspond to the apparent  $\beta$  relaxation. Figure 4 shows the mixing enthalpy of the constituents of the  $(La_{0.5}Ce_{0.5})_{65}Al_{10}(Co_xCu_{1-x})_{25}$  at% ( $x = 0, 0.2, 0.4, 0.6, \text{ and } 0.8$ ) metallic glasses (The data of mixing enthalpy are derived from the reference [35]). The mixing enthalpy  $\Delta H_m$  of the “solvent” atoms, La/Ce, with the “solute” atoms are almost identical:  $\Delta H_m$  (La/Ce-Al) =  $-38$  kJ/mol,  $\Delta H_m$  (La/Ce-Cu) =  $-21$  kJ/mol,  $\Delta H_m$  (La-Co) =  $-17$  kJ/mol and  $\Delta H_m$  (La-Cu) =  $-18$  kJ/mol, reflecting the chemical similar chemistry of the rare-earth elements. As for the “solute” atoms, the mixing enthalpy of Cu-Co is positive, 6 kJ/mol, and the main difference appears when comparing the mixing enthalpies of Al-Cu,  $-1$  kJ/mol, to that of Al-Co,  $-18$  kJ/mol. Based on the empirical rules to determine  $\Delta H_{mix}$ , the mixing enthalpy of  $(La_{0.5}Ce_{0.5})_{65}Al_{10}(Co_xCu_{1-x})_{25}$  at% ( $x = 0, 0.2, 0.4, 0.6, 0.8$ ) metallic glasses is given in Figure 4. We observed an actual decrease of the enthalpy of mixing as the concentration of Co increases. However, due to substitution of Cu by Co, the fluctuation on mixing enthalpies decreases, as the Al-Co mixing enthalpy is substantially more negative than that of Al-Cu and similar to those of La/Ce-Cu. According to the literature, this reduction on the mixing enthalpy fluctuation enhances the  $\beta$  relaxation [27].

Previous works proved that relaxation is connected to dynamic heterogeneity in glasses and related to the local movement of “weak spots” [36]. In particular, the microstructure inhomogeneity of metallic glass has been proven by means of microscopy and simulation [37].

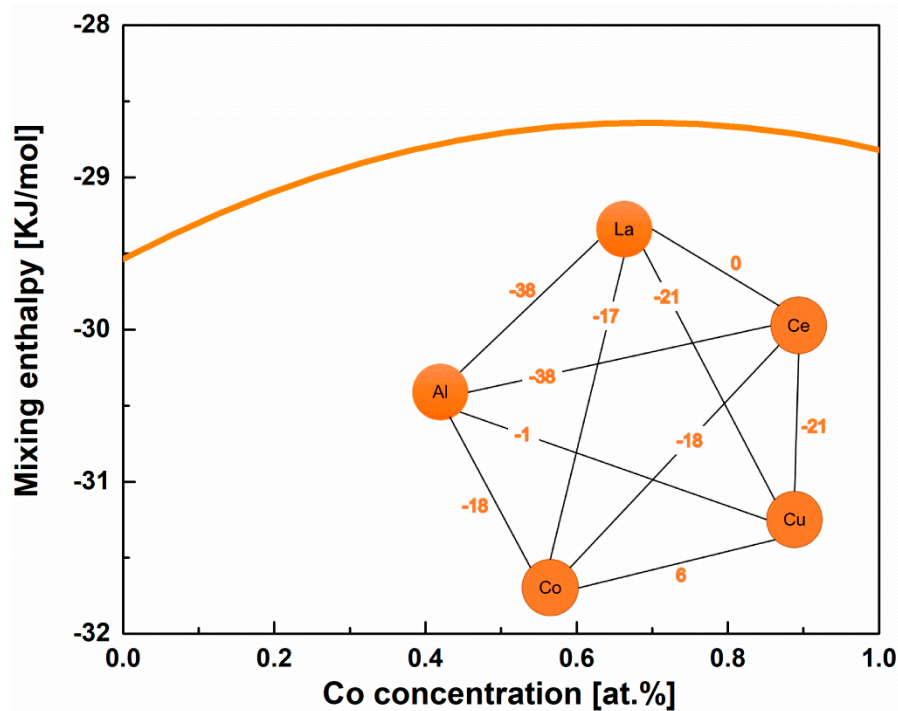


**Figure 4.** Mixing enthalpy of the  $(\text{La}_{0.5}\text{Ce}_{0.5})_{65}\text{Al}_{10}(\text{Co}_x\text{Cu}_{1-x})_{25}$  at% ( $x = 0, 0.2, 0.4, 0.6,$  and  $0.8$ ) metallic glasses. The inset displays the mixing enthalpy of constituent atoms (the data are taken from the reference [35]).

### 3.2.2. Physical Aging on the Secondary Relaxation of LaCe-Based Metallic Glass

From the thermodynamics point of view, annealing below the  $T_g$  drives the glassy state towards a more stable state of lower energy. Figure 5 presents the storage and loss factor of  $(\text{La}_{0.5}\text{Ce}_{0.5})_{65}\text{Al}_{10}(\text{Co}_{0.8}\text{Cu}_{0.2})_{25}$  metallic glass after annealing at 363 K for 24 h, which certainly illustrates that the intensity of the  $\beta$  relaxation reduces by physical aging below  $T_g$ .

As proposed in previous works, the  $\beta$  relaxation of metallic glasses is ascribed to the structural heterogeneity or local motion of the “defects” [1,33]. These defects are denominated as flow units [33,38], quasi-point defects (QPDs) [39], liquid-like sites [40], weakly bonded zones or loose packing regions [41]. According to Figure 5, annealing below the glass transition temperature can lead to disappearance of “defects” in metallic glasses. Physical aging causes rearrangement of atoms, resulting in an increase of density and elastic modulus. In the metallic glass, the mobility of atoms is closely related to “defects” concentration. Annealing causes the metallic glass to evolve towards a higher density state with a consequent reduction of the local “free volume” available for atomic rearrangement. Subsequent cooling after the annealing does not alter the glassy state, since the cooling rate is much lower than in the initial production of the glass.

In addition, physical aging below the glass transition temperature  $T_g$  leads to enthalpy relaxation of glassy materials. Figure 6 shows the DSC trace of the  $(\text{La}_{0.5}\text{Ce}_{0.5})_{65}\text{Al}_{10}(\text{Co}_{0.8}\text{Cu}_{0.2})_{25}$  metallic glass annealed at 363 K for 24 h. Comparison to the as-produced sample allows the identification of a notable enthalpy recovery, a consequence of the glass relaxation during annealing.

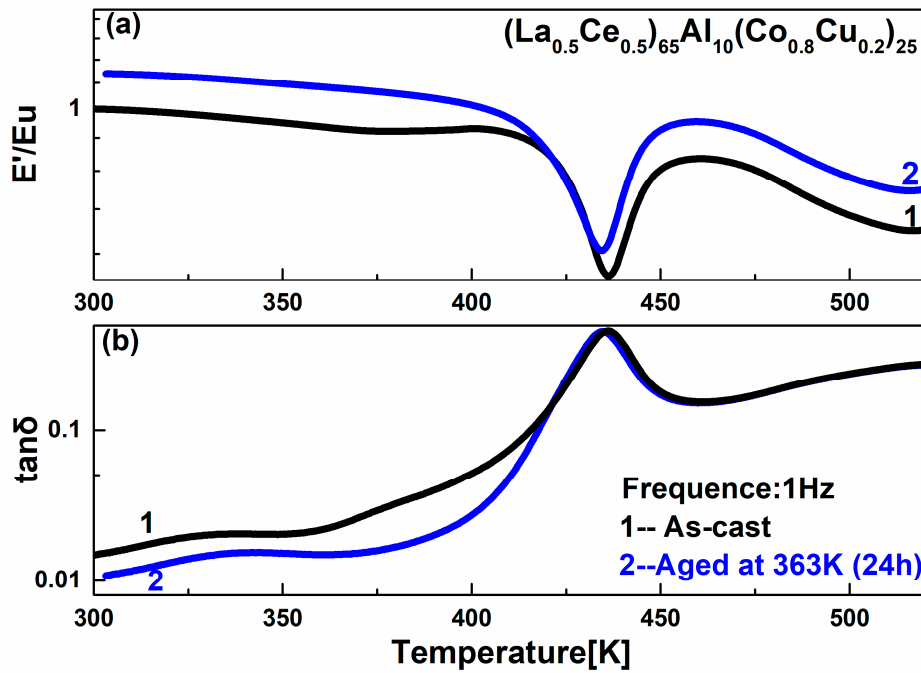


**Figure 5.** Temperature dependence of the normalized storage modulus (a) and loss factor (b) of  $(La_{0.5}Ce_{0.5})_{65}Al_{10}(Co_{0.8}Cu_{0.2})_{25}$  metallic glass (heating rate: 3 K/min and frequency: 0.3 Hz) (1) As-cast (2) annealed one (annealing temperature: 363 K and annealing time: 24 h).

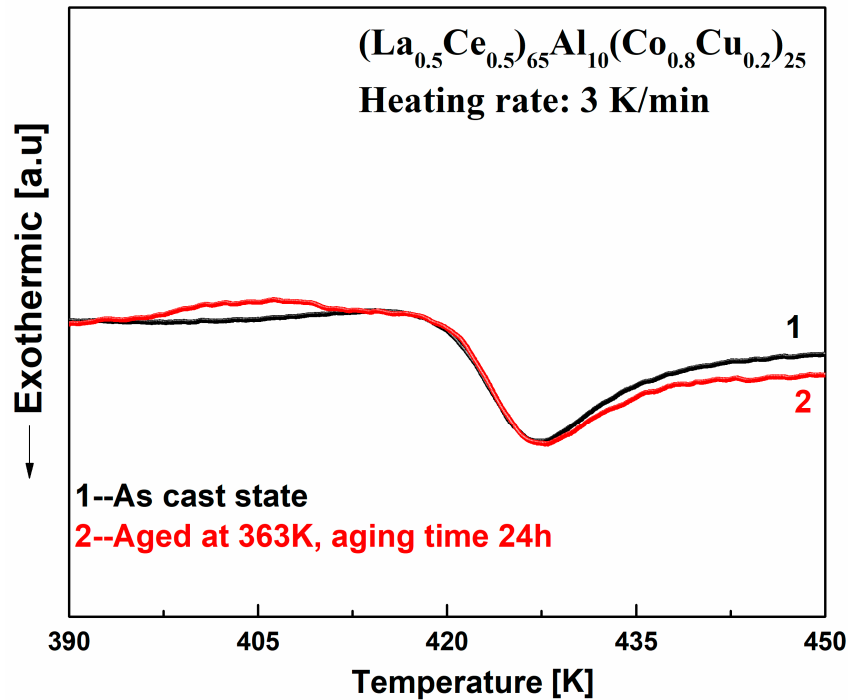


**Figure 6.** Enthalpy relaxation in  $(La_{0.5}Ce_{0.5})_{65}Al_{10}(Co_{0.8}Cu_{0.2})_{25}$  metallic glass bulk metallic glasses after aging at 363 K.

The structural relaxation observed in the DMA test can be analyzed by the growth of the loss factor ( $\tan\delta = E''/E'$ ) [42,43]. Figure 7 shows the loss factor ( $\tan\delta$ ) evolution versus annealing time in the  $(La_{0.5}Ce_{0.5})_{65}Al_{10}(Co_{0.8}Cu_{0.2})_{25}$  bulk metallic glass at 363 K. Previous works have characterized the

structural relaxation below  $T_g$  in amorphous materials, particularly in bulk metallic glasses, by using the Kohlrausch–Williams–Watts (KWW) equation [9,44].

$$\tan \delta(t_a) - \tan \delta(t_a = 0) = A\{1 - e^{[-(\frac{t_a}{\tau})^{\beta_{aging}}]}\} \quad (1)$$

where  $A = \tan \delta(t_a \rightarrow \infty) - \tan \delta(t_a = 0)$  is the maximum value of the dynamic relaxation.  $\tau$  is the relaxation time, and  $\beta_{aging}$  is the Kohlrausch exponent with values between 0 and 1. The best fit of Equation (1) to the data on the loss factor of the  $(La_{0.5}Ce_{0.5})_{65}Al_{10}(Co_{0.8}Cu_{0.2})_{25}$  metallic glass was obtained with  $\tau = 10,594$  s and  $\beta_{aging} = 0.4$ .

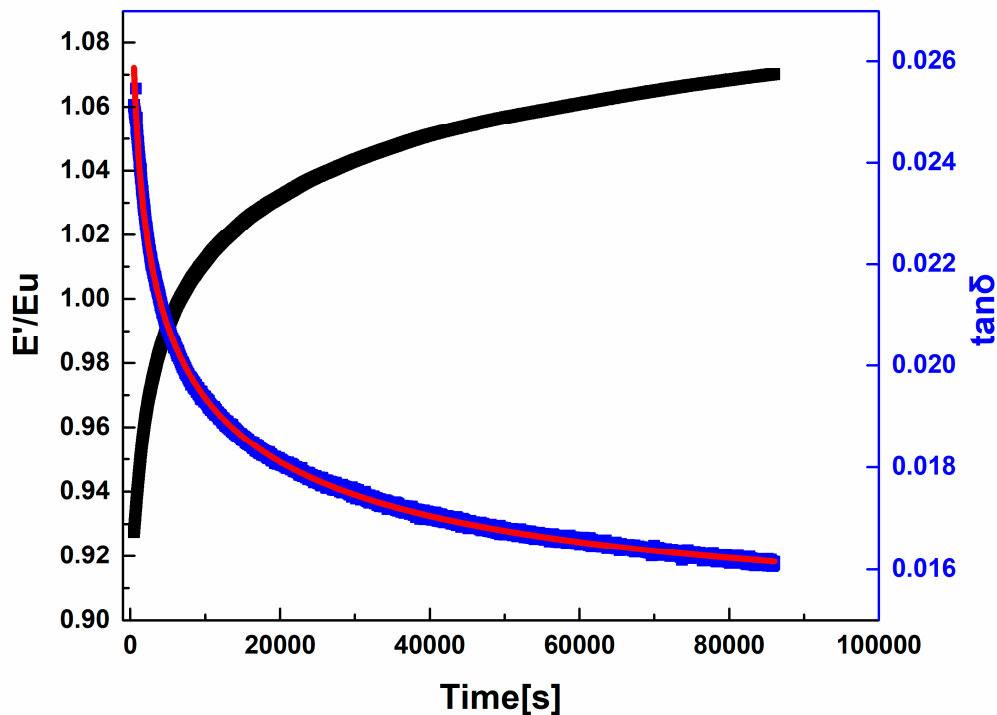


**Figure 7.** Evolution of the storage modulus  $E'$  and loss factor  $\tan \delta$  for  $(La_{0.5}Ce_{0.5})_{65}Al_{10}(Co_{0.8}Cu_{0.2})_{25}$  metallic glass with the annealing time. The aging temperature is  $T_a = 363$  K, and the driving frequency is 1 Hz. The red curve is the best fit from Equation (1) obtained for the parameters  $\tau = 10,594$  s and  $\beta_{aging} = 0.4$ .

The Kohlrausch exponent  $\beta_{KWW}$  reveals the presence of a broad distribution of relaxation times in the glass, with  $\beta_{KWW} = 1$  corresponding to a single Debye relaxation time.

Experimental values of the parameter  $\beta_{KWW}$  in amorphous alloys are in the range of 0.24–1 [45]. For amorphous polymers, values extend from 0.24 (polyvinyl chloride) to 0.55 (polyisobutylene), for alcohols from 0.45 to 0.75, while for orientational glasses and networks values are up to 1. In bulk metallic glasses, it appears that  $\beta_{KWW}$  is related to the fragility of the amorphous materials [42]. Values of  $\beta_{KWW}$  close to 1 indicate that the system is a strong glass former while values less than 0.5 suggest that the glass is a fragile glass [46,47]. According to the available literature, no defined trend characterizes the stretching parameters  $\beta_{KWW}$  in bulk metallic glasses, as it is either temperature dependent or temperature independent [48–50]. For example,  $Pd_{42.5}Ni_{7.5}Cu_{30}P_{20}$  bulk metallic glass has very similar fragility parameters,  $59 < m < 67$ , and similar stretched exponents,  $0.59 < \beta_{KWW} < 0.6$  [44]. However, experimental data indicate that the Kohlrausch exponent  $\beta_{aging}$  is around 0.4 for temperatures close to  $T_g$  [44], as found in the present case.

As proposed by Wang et al. [51], the kinetic parameter  $\beta_{KWW}$  is associated with the dynamic heterogeneity. The  $\beta_{KWW}$  parameter takes low values when the temperature is below the  $\beta$  relaxation

peak and increases dramatically when the temperature surpasses the glass transition temperature. The  $\beta$  relaxation in metallic glasses is related to the reversible displacement of the “defects”. When the stress relaxation is performed around the  $\beta$  relaxation temperature, only a small fraction of atoms are allowed to move. Thus, it can be concluded that lower  $\beta_{KWW}$  values around the  $\beta$  relaxation are ascribed to reversible “defects”.

#### 4. Conclusions

The dynamic mechanical properties of LaCe-based bulk metallic glasses were investigated by dynamic mechanical analysis. The experimental results reveal that the mechanical and thermal properties strongly depend on chemical composition. Substitution of Cu by Co enhances  $\beta$  relaxation due to the reduction of the enthalpy of mixing fluctuation. Physical aging below the glass transition temperature  $T_g$  reduces the concentration of local “defects” in metallic glasses and causes a decrease of the intensity for the  $\beta$  process. The curves of loss modulus can be well fitted by the KWW model, the fitting parameter  $\beta_{KWW}$  is approximately 0.4, indicating that the plastic deformation of the  $(\text{La}_{0.5}\text{Ce}_{0.5})_{65}\text{Al}_{10}(\text{Co}_{0.8}\text{Cu}_{0.2})_{25}$  metallic glass is related to the microstructural heterogeneity.

**Author Contributions:** M.L., Q.H. and Y.C. conducted the experiments and analyzed the experimental results. Q.H. and M.L. contributed to the sample preparation. M.L., J.Q., D.C., Y.Y. and J.-M.P. proposed the idea of the work, originated the experiment and write the paper.

**Funding:** This research was funded by the Fundamental Research Funds for the Central Universities (Nos. 3102018ZY010, 3102019ghxm007 and 3102017JC01003), Astronautics Supporting Technology Foundation of China (2019-HT-XG) and the Natural Science Foundation of Shaanxi Province (No. 2019JM-344). The investigation of Y.H. Chen and M.N. Liu sponsored by the Seed Foundation of Innovation and Creation for Graduate Students in Northwestern Polytechnical University (No. ZZ2019014). D. Crespo acknowledges financial support from MINECO, Spain, grant FIS2017-82625-P, and Generalitat de Catalunya, grant 2017SGR0042.

**Conflicts of Interest:** The authors declare no conflict of interest.

#### References

1. Qiao, J.C.; Wang, Q.; Pelletier, J.M.; Kato, H.; Casalini, R.; Crespo, D.; Pineda, E.; Yao, Y.; Yang, Y. Structural heterogeneities and mechanical behavior of amorphous alloys. *Prog. Mater. Sci.* **2019**, *104*, 250–329. [[CrossRef](#)]
2. Hufnagel, T.C.; Schuh, C.A.; Falk, M.L. Deformation of metallic glasses: recent developments in theory, simulations, and experiments. *Acta Mater.* **2016**, *109*, 375–393. [[CrossRef](#)]
3. Wang, W.H. The elastic properties, elastic models and elastic perspectives of metallic glasses. *Prog. Mater. Sci.* **2012**, *57*, 487–656. [[CrossRef](#)]
4. Inoue, A. Stabilization of metallic supercooled liquid and bulk amorphous alloys. *Acta Mater.* **2000**, *48*, 279–306. [[CrossRef](#)]
5. Sun, B.A.; Wang, W.H. The fracture of bulk metallic glasses. *Prog. Mater. Sci.* **2015**, *74*, 211–307. [[CrossRef](#)]
6. Qiao, J.C.; Chen, Y.H.; Casalini, R.; Pelletier, J.M.; Yao, Y. Main relaxation and slow relaxation processes in a  $\text{La}_{30}\text{Ce}_{30}\text{Al}_{15}\text{Co}_{25}$  metallic glass. *J. Mater. Sci. Technol.* **2019**, *35*, 982–986. [[CrossRef](#)]
7. Zhang, L.-C.; Jia, Z.; Lyu, F.; Liang, S.-X.; Lu, J. A review of catalytic performance of metallic glasses in wastewater treatment: Recent progress and prospects. *Prog. Mater. Sci.* **2019**, *105*, 100576. [[CrossRef](#)]
8. Jia, Z.; Wang, Q.; Sun, L.; Wang, Q.; Zhang, L.-C.; Wu, G.; Luan, J.-H.; Jiao, Z.-B.; Wang, A.; Liang, S.-X.; et al. Attractive in situ self-reconstructed hierarchical gradient structure of metallic glass for high efficiency and remarkable stability in catalytic performance. *Adv. Funct. Mater.* **2019**, *29*, 1807857. [[CrossRef](#)]
9. Qiao, J.C.; Pelletier, J.M. Dynamic mechanical relaxation in bulk metallic glasses: A review. *J. Mater. Sci. Technol.* **2014**, *30*, 523–545. [[CrossRef](#)]
10. Schuh, C.A.; Hufnagel, T.C.; Ramamurty, U. Mechanical behavior of amorphous alloys. *Acta Mater.* **2007**, *55*, 4067–4109. [[CrossRef](#)]
11. Wang, Q.; Liu, J.J.; Ye, Y.F.; Liu, T.T.; Wang, S.; Liu, C.T.; Lu, J.; Yang, Y. Universal secondary relaxation and unusual brittle-to-ductile transition in metallic glasses. *Mater. Today* **2017**, *20*, 293–300. [[CrossRef](#)]
12. Ghidelli, M.; Gravier, S.; Blandin, J.J.; Djemia, P.; Mompioni, F.; Abadias, G.; Raskin, J.P.; Pardoën, T. Extrinsic mechanical size effects in thin ZrNi metallic glass films. *Acta Mater.* **2015**, *90*, 232–241. [[CrossRef](#)]

13. Ghidelli, M.; Idrissi, H.; Gravier, S.; Blandin, J.-J.; Raskin, J.-P.; Schryvers, D.; Pardoën, T. Homogeneous flow and size dependent mechanical behavior in highly ductile Zr<sub>65</sub>Ni<sub>35</sub> metallic glass films. *Acta Mater.* **2017**, *131*, 246–259. [[CrossRef](#)]
14. Han, Z.; Wu, W.F.; Li, Y.; Wei, Y.J.; Gao, H.J. An instability index of shear band for plasticity in metallic glasses. *Acta Mater.* **2009**, *57*, 1367–1372. [[CrossRef](#)]
15. Leuzzi, L.; Nieuwenhuizen, T.M. Thermodynamics of the glassy state. *J. Stat. Phys.* **2008**, *133*, 1185–1186.
16. Dixon, P.K.; Lei, W.; Nagel, S.R.; Williams, B.D.; Carini, J.P. Scaling in the relaxation of supercooled liquids. *Phys. Rev. Lett.* **1990**, *65*, 1108–1111. [[CrossRef](#)]
17. Ngai, K.; Wang, Z.; Gao, X.; Yu, H.; Wang, W. A connection between the structural  $\alpha$ -relaxation and the  $\beta$ -relaxation found in bulk metallic glass-formers. *J. Chem. Phys.* **2013**, *139*, 014502. [[CrossRef](#)]
18. Qiao, J.C.; Wang, Q.; Crespo, D.; Yang, Y.; Pelletier, J.M. Amorphous physics and materials: Secondary relaxation and dynamic heterogeneity in metallic glasses: A brief review. *Chin. Phys. B* **2017**, *26*, 016402. [[CrossRef](#)]
19. Angell, C.A. Formation of glasses from liquids and biopolymers. *Science* **1995**, *267*, 1924–1935. [[CrossRef](#)]
20. Debenedetti, P.G.; Stillinger, F.H. Supercooled liquids and the glass transition. *Nature* **2001**, *410*, 259–267. [[CrossRef](#)]
21. Zhao, Z.; Wen, P.; Shek, C.; Wang, W. Measurements of slow  $\beta$ -relaxations in metallic glasses and supercooled liquids. *Phys. Rev. B* **2007**, *75*, 174201. [[CrossRef](#)]
22. Johari, G.P.; Goldstein, M. Viscous liquids and the glass transition. II. Secondary relaxations in glasses of rigid molecules. *J. Chem. Phys.* **1970**, *53*, 2372–2388.
23. Ngai, K.L.; Rendell, R.W. Cooperative dynamics in relaxation: A coupling model perspective. *J. Mol. Liq.* **1993**, *56*, 199–214. [[CrossRef](#)]
24. Kudlik, A.; Benkhof, S.; Blochowicz, T.; Tschirwitz, C.; Rössler, E. The dielectric response of simple organic glass formers. *J. Mol. Struct.* **1999**, *479*, 201–218. [[CrossRef](#)]
25. Qiao, J.C.; Wang, Y.-J.; Pelletier, J.M.; Keer, L.M.; Fine, M.E.; Yao, Y. Characteristics of stress relaxation kinetics of La<sub>60</sub>Ni<sub>15</sub>Al<sub>25</sub> bulk metallic glass. *Acta Mater.* **2015**, *98*, 43–50. [[CrossRef](#)]
26. Lyu, G.J.; Qiao, J.C.; Pelletier, J.M.; Yao, Y. The dynamic mechanical characteristics of Zr-based bulk metallic glasses and composites. *Mater. Sci. Eng., A* **2018**, *711*, 356–363. [[CrossRef](#)]
27. Qiao, J.C.; Yao, Y.; Pelletier, J.M.; Keer, L.M. Understanding of micro-alloying on plasticity in Cu<sub>46</sub>Zr<sub>47-x</sub>Al<sub>7</sub>Dy<sub>x</sub> (0 ≤ x ≤ 8) bulk metallic glasses under compression: Based on mechanical relaxations and theoretical analysis. *Int. J. Plast.* **2016**, *82*, 62–75. [[CrossRef](#)]
28. Yao, Z.F.; Qiao, J.C.; Pelletier, J.M.; Yao, Y. Characterization and modeling of dynamic relaxation of a Zr-based bulk metallic glass. *J. Alloys Compd.* **2017**, *690*, 212–220. [[CrossRef](#)]
29. Qiao, J.C.; Casalini, R.; Pelletier, J.M.; Yao, Y. Dynamics of the strong metallic glass Zn<sub>38</sub>Mg<sub>12</sub>Ca<sub>32</sub>Yb<sub>18</sub>. *J. Non-Cryst. Solids* **2016**, *447*, 85–90. [[CrossRef](#)]
30. Yu, H.B.; Wang, W.H.; Bai, H.Y.; Samwer, K. The  $\beta$ -relaxation in metallic glasses. *Natl. Sci. Rev.* **2014**, *1*, 429–461. [[CrossRef](#)]
31. Yu, H.B.; Shen, X.; Wang, Z.; Gu, L.; Wang, W.H.; Bai, H.Y. Tensile plasticity in metallic glasses with pronounced  $\beta$  relaxations. *Phys. Rev. Lett.* **2012**, *108*, 015504. [[CrossRef](#)]
32. Ichitsubo, T.; Matsubara, E.; Yamamoto, T.; Chen, H.S.; Nishiyama, N.; Saida, J.; Anazawa, K. Microstructure of fragile metallic glasses inferred from ultrasound-accelerated crystallization in Pd-based metallic glasses. *Phys. Rev. Lett.* **2005**, *95*, 245501. [[CrossRef](#)]
33. Wang, W.H. Dynamic relaxations and relaxation-property relationships in metallic glasses. *Prog. Mater. Sci.* **2019**, *106*, 100561. [[CrossRef](#)]
34. Yu, H.B.; Samwer, K.; Wang, W.H.; Bai, H.Y. Chemical influence on  $\beta$ -relaxations and the formation of molecule-like metallic glasses. *Nat. Commun.* **2013**, *4*, 1345–1346.
35. Takeuchi, A.; Inoue, A. Classification of bulk metallic glasses by atomic size difference, heat of mixing and period of constituent elements and its application to characterization of the main alloying element. *Mater. Trans.* **2005**, *46*, 2817–2829. [[CrossRef](#)]
36. Liu, S.T.; Wang, Z.; Peng, H.L.; Yu, H.B.; Wang, W.H. The activation energy and volume of flow units of metallic glasses. *Scr. Mater.* **2012**, *67*, 9–12. [[CrossRef](#)]

37. Liu, Y.H.; Wang, D.; Nakajima, K.; Zhang, W.; Hirata, A.; Nishi, T.; Inoue, A.; Chen, M.W. Characterization of nanoscale mechanical heterogeneity in a metallic glass by dynamic force microscopy. *Phys. Rev. Lett.* **2011**, *106*, 125504. [[CrossRef](#)]
38. Liu, S.T.; Jiao, W.; Sun, B.A.; Wang, W.H. A quasi-phase perspective on flow units of glass transition and plastic flow in metallic glasses. *J. Non-Cryst. Solids* **2013**, *376*, 76–80. [[CrossRef](#)]
39. Perez, J.; Etienne, S.; Tatibouât, J. Determination of glass transition temperature by internal friction measurements. *Phys. Status Solidi a* **1990**, *121*, 129–138. [[CrossRef](#)]
40. Egami, T. Mechanical failure and glass transition in metallic glasses. *J. Alloys Compd.* **2011**, *509*, S82–S86. [[CrossRef](#)]
41. Qiao, J.C.; Pelletier, J.M. Kinetics of structural relaxation in bulk metallic glasses by mechanical spectroscopy: Determination of the stretching parameter  $\beta_{KWW}$ . *Intermetallics* **2012**, *28*, 40–44. [[CrossRef](#)]
42. Qiao, J.; Pelletier, J.M.; Casalini, R. Relaxation of bulk metallic glasses studied by mechanical spectroscopy. *J. Phys. Chem. B* **2013**, *117*, 13658–13666. [[CrossRef](#)]
43. Pelletier, J.M. Influence of structural relaxation on atomic mobility in a  $Zr_{41.2}Ti_{13.8}Cu_{12.5}Ni_{10.0}Be_{22.5}$  (Vit1) bulk metallic glass. *J. Non-Cryst. Solids* **2008**, *354*, 3666–3670.
44. Qiao, J.; Casalini, R.; Pelletier, J.M.; Kato, H. Characteristics of the structural and Johari–Goldstein Relaxations in Pd-based metallic glass-forming liquids. *J. Phys. Chem. B* **2014**, *118*, 3720–3730. [[CrossRef](#)]
45. Böhmer, R.; Ngai, K.L.; Angell, C.A.; Plazek, D.J. Nonexponential relaxations in strong and fragile glass formers. *J. Chem. Phys.* **1993**, *99*, 4201–4209. [[CrossRef](#)]
46. Angell, A.C. Relaxation in liquids, polymers and plastic crystals—Strong/fragile patterns and problems. *J. Non-Cryst. Solids* **1991**, *131–133*, 13–31. [[CrossRef](#)]
47. Raghavan, R.; Murali, P.; Ramamurty, U. Influence of cooling rate on the enthalpy relaxation and fragility of a metallic glass. *Metall. Mater. Trans. A* **2008**, *39*, 1573–1577. [[CrossRef](#)]
48. Zhang, Y.; Hahn, H. Study of the kinetics of free volume in  $Zr_{45.0}Cu_{39.3}Al_{17.0}Ag_{8.7}$  bulk metallic glasses during isothermal relaxation by enthalpy relaxation experiments. *J. Non-Cryst. Solids* **2009**, *355*, 2616–2621.
49. Zhang, T.; Ye, F.; Wang, Y.; Lin, J. Structural Relaxation of  $La_{55}Al_{25}Ni_{10}Cu_{10}$  bulk metallic glass. *Metall. Mater. Trans. A* **2008**, *39*, 1953–1957. [[CrossRef](#)]
50. Gallino, I.; Shah, M.B.; Busch, R. Enthalpy relaxation and its relation to the thermodynamics and crystallization of the  $Zr_{58.5}Cu_{15.6}Ni_{12.8}Al_{10.3}Nb_{2.8}$  bulk metallic glass-forming alloy. *Acta Mater.* **2007**, *55*, 1367–1376.
51. Wang, Z.; Sun, B.A.; Bai, H.Y.; Wang, W.H. Evolution of hidden localized flow during glass-to-liquid transition in metallic glass. *Nat. Commun.* **2014**, *5*, 5823. [[CrossRef](#)]

